

## Na( $3p \leftarrow 3s$ ) excitation by impact of slow multiply charged ions

G. Horvath,<sup>1</sup> J. Schweinzer,<sup>2</sup> HP. Winter,<sup>1</sup> and F. Aumayr<sup>1,\*</sup>

<sup>1</sup>*Institut für Allgemeine Physik, Technische Universität Wien, Wiedner Hauptstraße 8-10, A-1040 Wien, Austria*

<sup>2</sup>*Max Planck Institut für Plasmaphysik, Boltzmannstrasse 2, D-85748 Garching, Germany*

(Received 28 February 1996)

We present a systematic experimental and theoretical study of Na( $3p \leftarrow 3s$ ) excitation by slow ( $v < 1$  a.u.) singly and multiply charged ions. In particular, the scaling behavior of the respective excitation cross section  $\sigma_{\text{NaI}}$  with projectile ion charge state  $q$  is investigated. Due to the dominance of the competing electron capture channels at low collision energies  $E$ , the excitation cross sections deviate significantly from a commonly applied  $\sigma/q = f(E/q)$  cross-section scaling relation. [S1050-2947(96)00310-1]

PACS number(s): 34.50.Fa

### I. INTRODUCTION

Plasma-wall interaction and impurity transport processes in the outermost region of magnetically confined hot plasmas (the so-called plasma edge) need to be well understood for successful development of future thermonuclear fusion reactors. Toward this goal, detailed edge plasma diagnostics are in great demand. By injecting a fast Li atom beam into the edge plasma region, an impressive amount of information can be obtained with excellent space and time resolution [1]. This so-called Li beam plasma spectroscopy gives access not only to the edge plasma density profiles from collisionally excited Li atoms [2,3], but also impurity ion concentration and temperature profiles can be obtained from characteristic line emission following electron capture from the injected Li atoms [4,5].

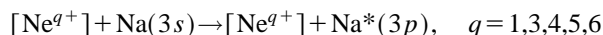
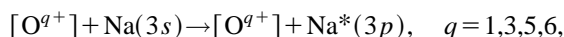
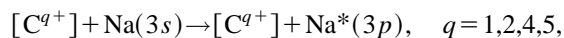
Full utilization of these capabilities requires a reliable database for the involved atomic collision processes between injected Li atoms and plasma constituents (i.e., electrons, hydrogen ions, and relevant impurities in different charge states). A precise modeling of the Li beam attenuation and excited-state composition is needed for evaluating plasma properties of interest from the spectroscopic measurements [1,2]. Recently, an atomic database was established, which contains evaluated experimental and theoretical cross sections [6]. Collision of Li atoms with, respectively, electrons and protons has been considered in a wide energy range, to describe the interaction of the injected Li beam with a clean hydrogen plasma.

However, in the plasma edge impurity ions are certainly non-negligible and thus have to be taken into account for accurate evaluation of diagnostic data [1,2]. There are calculated as well as experimental cross sections for single electron capture from alkali-metal atoms such as Li( $2s$ ) or Na( $3s$ ) by multicharged ions (cf. [7] and references therein), whereas alkali-metal-atom excitation by impact of multiply charged ions has been investigated mainly theoretically [7,8], with experimental results being only available for impact of

He<sup>2+</sup> on Li and Na [9,10]. Such target excitation (TX) in collisions of slow ( $v < 1$  a.u.) singly or multiply charged ions  $Z^{q+}$  with alkali-metal atoms is therefore both of fundamental and practical interest.

As exemplified for TX of atomic hydrogen, there is no general scaling relation at low impact energy [11]. A scaling of reduced cross sections  $\sigma/q$  with reduced impact energies  $E/q$  by Janev and Presnyakov [12] is restricted to impact energies  $E/q > 15$  keV/amu. This scaling has been verified for ions in various charge states in systematic experimental studies for H( $1^1S \rightarrow n^1P$ ) ( $n=2-6$ ) transitions and for He( $1^1S \rightarrow n^1L$ ,  $n=2-4$ ,  $L=S,P,D$ ) transitions at impact energies of 15–200  $q$  keV/amu [13–16]. These studies were mainly motivated by the important role of TX processes in attenuation of fast neutral heating beams for fusion plasmas. A recent, more general scaling introduced by Janev [17] for dipole-allowed as well as dipole-forbidden excitation (valid only for  $E/q > 25$  keV/amu) gives for fixed  $E$  nonscaled excitation cross sections that do not saturate toward high- $q$  values but rather decrease beyond a maximum obtained for certain  $q$ .

The present work as a combined experimental and theoretical study focuses on TX of Na( $3s$ ) atoms due to low-energy ( $E \leq 25$  keV/amu) impact of various  $Z^{q+}$  ions. Experimental investigations of the collision systems



at impact energies below 4 keV/amu have been performed by means of absolute photon spectroscopy of the respective NaD (589.0+589.6 nm) emission (the square brackets symbolize that neither primary nor secondary projectile states have been specified). Na has been chosen as a target for technical reasons only, but the excitation of Li( $2s-2p$ ) is believed to behave in a very similar way. Measurements are compared with large-scale atomic-orbital (AO) close-coupling calculations (AO-CC) involving bare nuclei (i.e., H<sup>+</sup>, He<sup>2+</sup>, Be<sup>4+</sup>) in place of the actually incompletely stripped projectiles. Since for single-electron capture (SEC) processes the relevant emission cross sections mainly depend

\*Author to whom correspondence should be addressed. Mailing address: Friedrich Aumayr, Institut für Allgemeine Physik, TU-Wien, A-1040 Vienna, Austria. FAX: (+43-1) 5864203. Electronic address: aumayr@iap.tuwien.ac.at

on the projectile ion charge rather than the detailed electronic structure of the projectile [18], present TX data calculated with fully stripped ions should also be relevant for incompletely stripped impurity ions of equal charge state  $q$ .

The outline of this paper is as follows. Our experimental and theoretical techniques will be described in Secs. II and III, respectively. The experimental results are presented in Sec. IV and compared with our theoretical results in Sec. V. Regarding beam diagnostics of fusion edge plasmas, special emphasis has been devoted to the scaling properties of TX emission cross sections.

## II. EXPERIMENTAL TECHNIQUE

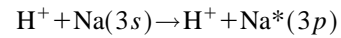
We used a crossed-beam apparatus similar to the one described in Refs. [19, 20]. Ions of interest were extracted from a 5-GHz ECR (electron cyclotron resonance) ion source [21], accelerated by up to 12 kV, focused by a magnetic quadrupole doublet, charge to mass separated by means of an analyzing magnet and directed into the collision chamber, wherein after passing the alkali-metal target atom beam (cf. below) the ions were collected in a Faraday cup.

The Na atom beam was produced by effusion from a Knudsen cell inside a heated oven (see Refs. [19, 22]) surrounded by radiation shields. An aperture provided collimation of the effusive beam, which could be stopped by means of a mechanical shutter to account for photon signals from excitation of residual gas molecules. After having passed the interaction region the alkali-metal atom beam was stopped by a water-cooled trap. Background pressure during measurements was typically  $10^{-6}$  mbar. Careful alignment of the oven assured that the ion and atom beam intersected each other precisely in the viewing line of the light collection system (see below). Single collision conditions were assured by monitoring the fraction of charge exchanged primary ions with and without target beam.

NaD (589.0+589.6 nm) line radiation from the ion-atom interaction region was detected free of polarization influences at the ‘‘magic’’ angle of  $54.7^\circ$  with respect to the ion beam axis, by a Peltier-cooled EMI-9893 QB/100 photomultiplier equipped with a Schott-type MA 7-0.5 interference filter. The observation lengths of the photon detection system were limited by slits to 6.5 mm along the ion beam axis, in order to reduce background from excitation of residual gas molecules or scattered Na atoms. The accumulation time for the photomultiplier counting signal was controlled by a data acquisition program that also covered recording and integration of the primary ion beam current up to a presettable charge, to become independent of primary ion beam fluctuations. Measuring cycles with ion—and/or Na atom—beams on and off, respectively, were performed for proper background discrimination.

As a first step, relative courses of the NaD emission cross sections with ion impact energy have been determined. In these measurements the stability of the alkali-metal beam target was checked by repeatedly taking data at the specific impact energy of 4.5  $q$  keV.

In a second step, calibration of the relative data was obtained by comparing photon signals produced by ions of present interest to those produced by proton impact excitation,



at 4.5-keV impact energy and under the same observation geometry, making use of our previously determined absolute NaD emission cross sections for the latter collision system [22].

Our relative cross sections involve statistical errors (mainly due to counting statistics and Na target fluctuations) of typically  $\pm 5\%$  for ion beams in low charge states (singly and doubly charged ions), and up to  $\pm 20\%$  for ion beams in higher charge states. For the absolute cross-section data the quoted error of the reference cross section ( $\pm 25\%$ ) has to be taken care of in addition to the uncertainty of our relative measurements, leading to total errors of about  $\pm 25\text{--}32\%$ . In principle, our measured NaI ( $3s \leftarrow 3p$ ) emission cross sections differ from the respective Na( $3p$ ) excitation cross sections because of possible cascade contributions to the population of  $\text{Na}^*(3p)$  from higher  $\text{Na}(n, l)$  levels excited in the collision. Our AO-CC calculations (cf. Sec. III) indicate that in some cases cascading especially from  $\text{Na}(3d)$  can contribute to the measured emission cross section by up to 20%. However, no further attempt has been made to account for this influence.

## III. AO CALCULATIONS

In the present work we adopt the semiclassical impact-parameter formulation of the close-coupling method, assuming straight line trajectories for the projectiles. The time-dependent electronic wave function is expanded in projectile and target centered traveling orbitals, which need not necessarily be eigenstates of the corresponding atomic Hamiltonians. Thus, besides atomic orbitals also so-called pseudostates (PS) are included in our two-center expansion model. Whereas AO represent the bound spectrum of the separated atoms (SA) of relevance for the considered inelastic collision process, PS are chosen to account for the formation of transient molecular orbitals at small internuclear distances and/or low impact energies. The inclusion of states of the united atom (UA) on both collision centers has proven to extend the range of applicability of the AO-CC method towards lower impact energies and to improve the determination of subshell cross sections in general [23].

The CC calculation always starts from a linear combination of orbitals that result from diagonalization of the atomic Hamiltonians within the given set of basis states on each center. Linear combinations with negative eigenvalues correspond to the bound states, and states with positive energies are taken as representations of the continua of target and projectile, respectively. All states included in the presented CC calculation have been listed in Table I. The projectile ( $Z^{q+} = \text{H}^+, \text{He}^{2+}, \text{Be}^{4+}$ ) centered part of the basis consists not only of exact hydrogenlike states for ion charge  $z = q$  describing SEC reaction channels but also of hydrogen orbitals with charges  $z = q + 1$ , which correspond to states of the respective UA.

The interaction between the  $\text{Na}^+$  core and the ‘‘active’’ electron is described by a model potential of Rapp and Chang [24]. The radial parts of the corresponding eigenstates are expressed by linear combinations of Slater-type orbitals (STO). In addition, hydrogen orbitals with charges  $z = q + 1$  that correspond to states of the UA are also in-

TABLE I. Basis sets used in CC calculations to describe low-energy excitation in  $Z^{q+}$  ( $Z=H, He, Be$ ;  $q=1,2,4$ )– $Na(3s)$  collisions. For distinction between atomic orbital (AO) and pseudostates (PS), all states on both centers are given for each CC calculation. Hydrogenic orbitals are designated by the principal quantum number  $n$ , the angular momentum  $l$ , and the charge  $z$ , respectively. No specification of  $l$  means the full set of  $l$  quantum numbers for a given  $n$ . Slater-type orbitals (1-STO) are used to build up the Na atomic orbitals. The STO parameters can be found in Rapp and Chang [24], as well as the used pseudopotential. In all cases the full set of  $m$  quantum numbers is included in the basis. The calculations are specified by the number of states defined on the projectile and on the target center, respectively.

CC calculations	Center on projectile		Center on Na	
	AO	PS	AO	PS
$H^+$				
AO16-18	$n=1,2,3$	$z=2: n=3$	$3s,3p,3d,$ $4s,4p$	$4s$ -STO, $1p$ -STO; $z=2: 3d$
$He^{2+}$				
AO29-21	$n=3$	$z=3: n=3,4,$ $5d,5f$	$3s,3p$	$2s$ -STO; $z=3: n=3,4$
AO49-18	$n=2,3,4,5$	$z=3: n=4,$ $5g$	$3s,3p,3d,$ $4s,4p$	$4s$ -STO, $1p$ -STO; $z=2: 3d$
$Be^{4+}$				
AO40-30	$n=4,5,6$ ( $l \leq 4$ )		$3s,3p$	$2s$ -STO; $z=5: n=5,6$ ( $l \leq 3$ )
AO50-42	$n=1,2,3,4,5$	$z=5: 5f,5g,6h$	$3s,3p,3d,4s,4p$	$4s$ -STO, $1p$ -STO $z=5: n=3,4$ ( $l \geq 1$ ), $5$ ( $l \geq 2$ )

cluded on the target centered part of the expansion.

One-center couplings between projectile states induced by the electric field of the  $Na^+$  core are calculated in good approximation by assuming a pure Coulomb interaction potential. All presented calculations have been performed in the so-called collision system. Since the excitation process in the low-energy range is quite complex, the reliability of such calculated excitation cross sections is of some concern. Excitation channels are populated only with small probabilities because of the strongly competing SEC channels. In such a situation the calculation of cross sections is not a trivial task, and large basis sets are required to describe properly the nondominant excitation process. Therefore, besides the presented calculations given in Table I, we have performed additional studies with smaller basis sets to estimate the sensitivity of the calculated cross sections with respect to the chosen basis. Results of CC calculations for impact energies  $E \leq 1$  keV/amu were very sensible to the choice of the basis. While the choice of basis states in a pure AO expansion is quite straightforward, the situation becomes more complicated when PS are also considered. Adding PS with the same  $l, m$  values as for the AO to an already large AO basis will not improve the convergence of such a calculation considerably at low impact energy. This is due to the fact that, after diagonalizing the set of states on each atomic center, the PS states included in addition to the AO are connected to energy eigenvalues that differ considerably from the initial binding energy of the active electron. Such states cannot be called “close coupled” anymore. Even transiently they are only weakly populated and produce a small effect on final results at low impact energies. Quite on the contrary, improvement will be gained by inclusion of PS states when the fraction of AO states in a basis is reduced to the most important ones, in order to introduce “close-coupled” PS states.

In addition, we have carefully checked the numerical accuracy of our cross sections by comparing calculations performed on different meshes of internuclear distance  $R$  and impact parameter  $b$ . These numerical errors have been kept below 2% for the highest and below 7% for the lowest impact energies, respectively. Altogether, we believe that the final cross sections are accurate within  $\pm 10\%$  for  $E > 1$  keV/amu and within  $\pm 20\%$  at lower impact energy. Further discussion about the basis sensitivity and accuracy of results calculated for various collision systems will be presented in Sec. V.

#### IV. PRESENTATION OF EXPERIMENTAL RESULTS

Our experimental results for NaD emission in  $Z^{q+}$ - $Na(3s)$  collisions (for  $Z=C, q=1,2,4,5$ ;  $O, q=1,3,5,6$ ;  $Ne, q=1,3,4,5,6$ ) are presented in Figs. 1–3, respectively, as a function of ion impact energy per atomic mass unit. The error bars shown do not include the uncertainty of the used reference cross section (cf. Sec. II).

As a general trend we note that the measured NaD emission cross sections do not strongly depend on projectile charge states and species (if compared at the same impact velocity or impact energy per atomic mass unit). However, a closer look reveals the fairly general trend that projectile ions in higher charge states are generally somewhat less efficient in exciting the alkali atoms than the lower charged ones. At first thought this seems somewhat unexpected, because higher charge states should exert a stronger Coulomb interaction. All cross sections exhibit pronounced oscillatory structures with no apparent regularity. To test the scaling proposed by Janev and Presnyakov [12], we have also plotted (not shown) our data as reduced cross sections  $\sigma/q$  versus reduced impact energy  $E/qm$ . However, this scaling (which

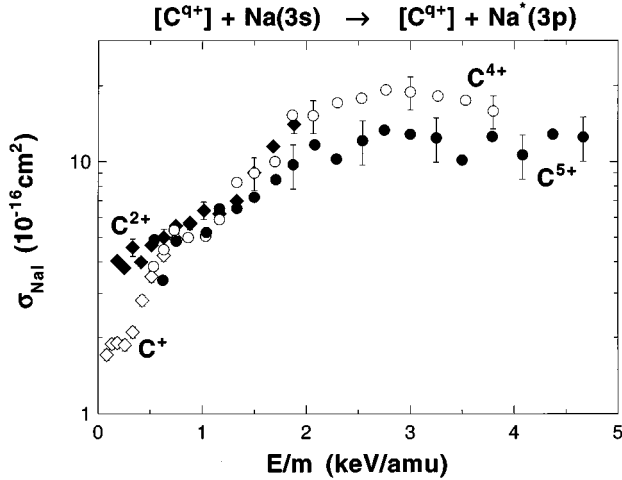


FIG. 1. Measured NaI (589.0+589.6 nm) emission cross sections for impact  $C^{q+}$  ( $q=1,2,4,5$ ) on  $Na(3s)$ , vs ion impact energy per atomic mass unit.  $\diamond$ :  $C^+$ ;  $\blacklozenge$ :  $C^{2+}$ ;  $\circ$ :  $C^{4+}$ ;  $\bullet$ :  $C^{5+}$ . Representative relative errors are shown (cf. text).

was mainly intended for  $E/q > 10$  keV/amu) proved inappropriate at our comparably low impact energies. A simple charge and species averaged cross section  $\sigma(E/m)$  as proposed by Schweinzer *et al.* [7] would represent a better “universal” excitation curve, e.g., for Li beam plasma spectroscopy (see the Introduction).

In the next section we make use of our AO calculations to interpret and discuss these experimental findings. We would like to point out, however, that effects of the electronic projectile structure, as seen in the experiment when comparing cross sections for different projectile species but same charge state  $q$ , are principally not covered by our calculations, which involve bare ions of the same charge state.

## V. THEORETICAL RESULTS AND DISCUSSION

First, we will compare our theoretical results for  $Na(3s-3p)$  excitation in collisions of  $Na(3s)$  atoms with “bare”  $Z^{q+}$  ( $q=1,2,4$ ) projectiles to our experimental data as well as

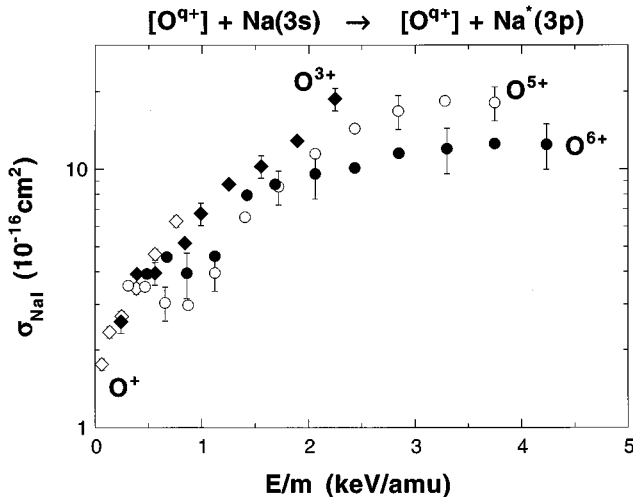


FIG. 2. Same as Fig. 1, but for impact of  $O^{q+}$  ( $q=1,3,5,6$ ).  $\diamond$ :  $O^+$ ;  $\blacklozenge$ :  $O^{3+}$ ;  $\circ$ :  $O^{5+}$ ;  $\bullet$ :  $O^{6+}$ .

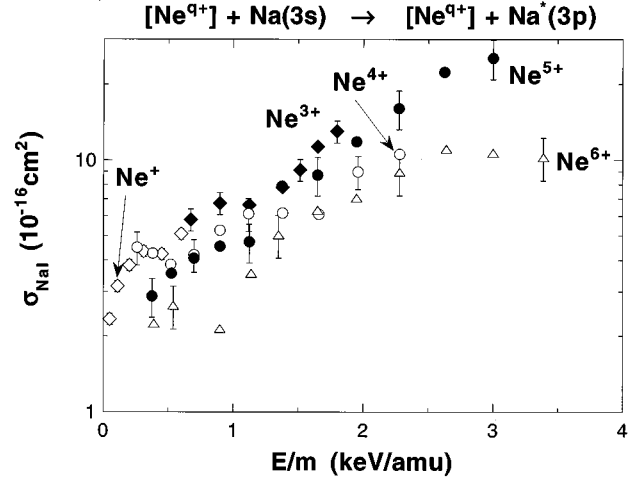


FIG. 3. As Fig. 1, but for impact of  $Ne^{q+}$  ( $q=1,3,4,5,6$ ).  $\diamond$ :  $Ne^+$ ;  $\blacklozenge$ :  $Ne^{3+}$ ;  $\circ$ :  $Ne^{4+}$ ;  $\bullet$ :  $Ne^{5+}$ ;  $\triangle$ :  $Ne^{6+}$ .

to data from other groups. Thereafter the question of scaling relations will be addressed. All AO calculations are specified by the number of states included on the projectile and on the  $Na^+$  center, respectively.

### A. $Z^+-Na(3s) \rightarrow Z^+-Na(3p)$

In Fig. 4 results from calculations employing different versions of the close-coupling approach [25–27] are compared. Excellent agreement between all theories can be stated. The systematically higher values of Jain and Winter [27] are due to the inclusion of cascade contributions to the cross section, thus presenting more an emission rather than a pure excitation cross section as all the other theoretical results. Our AO-CC results are very close to the values of Fritsch [26] and Shingal *et al.* [25]. However, at  $E \geq 4$  keV/amu our results tend to overestimate their cross sections.

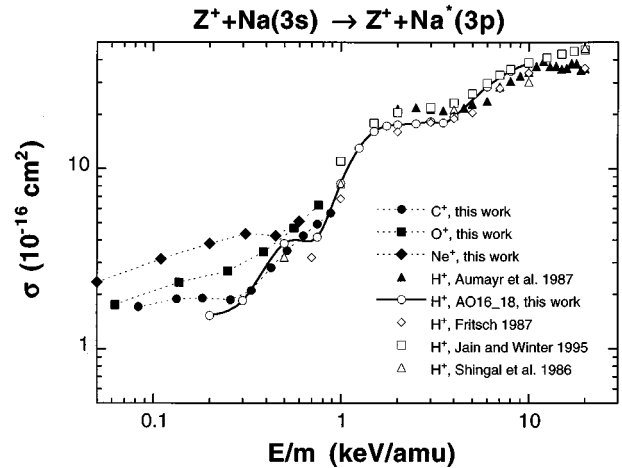


FIG. 4. Measured NaI (589.0+589.6 nm) emission and calculated  $Na(3p)$  excitation cross sections vs ion impact energy per atomic mass unit for impact of various singly charged ions. Experimental data ( $E$ ):  $\bullet$ :  $C^+$  (this work);  $\blacksquare$ :  $O^+$  (this work);  $\blacklozenge$ :  $Ne^+$  (this work);  $\blacktriangle$ :  $H^+$  (Ref. [22]). Calculated data ( $T$ ) are for  $H^+$  projectiles only:  $\circ$ : AO16-18 this work;  $\diamond$ : Ref. [26];  $\square$ : Ref. [27];  $\triangle$ : Ref. [25].

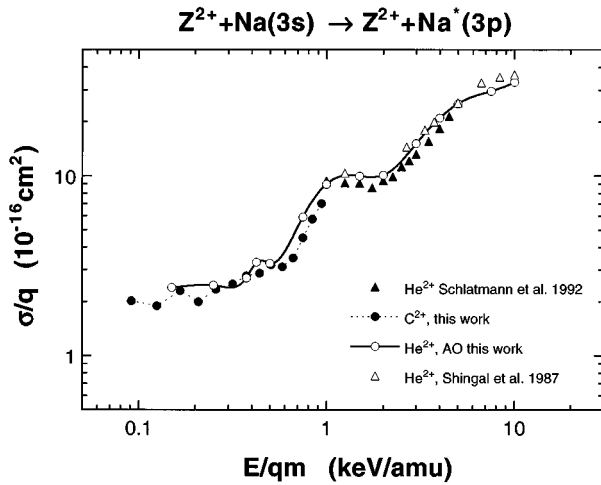


FIG. 5. Measured NaI (589.0+589.6 nm) emission and calculated Na(3*p*) excitation cross sections plotted as reduced cross section  $\sigma/q$  vs reduced impact energy  $E/qm$  for impact of various doubly charged ions. Experimental data ( $E$ ): ●:  $C^{2+}$  (this work); ▲:  $He^{2+}$  (Ref. [10]). Calculated data ( $T$ ) are for  $He^{2+}$  projectiles: ○: AO this work; △: Ref. [29].

This is due to neglecting continuum states representing ionization, which become important at these impact energies (cf. Table I for basis sets of AO16-18 calculation). However, it was our intention to optimize our basis by inclusion of low-lying PS, in order to describe TX at low impact energies.

Our experimental results for  $C^+$  projectiles as well as the experimental data of Aumayr *et al.* [22] for protons are in close agreement with all theoretical results. Increasing the number of core electrons in the projectile, however, also influences the TX cross section (cf. results for  $O^+$ ,  $Ne^+$  in Fig. 4). It is well known [28], and corresponds to our experience from AO-CC calculations, that at low impact energies all inelastic reaction channels are strongly coupled. Especially TX is suppressed by the dominant SEC process at such low collision velocities. Since SEC in collisions of singly charged ions with alkali-metal atoms strongly depends on the respective energy defect of the reaction and therefore on the specific electronic structure of the projectile, the strong coupling between SEC and TX channels also influences the TX cross section. This sensitivity on the projectile's electronic structure naturally decreases towards higher impact energies (cf. Fig. 4). Note that this explanation does not assume any direct electron-electron interaction in the TX process, which of course cannot be ruled out. From both theory and experiment a distinct "structure" in the TX cross section in the range  $1 < E < 4$  keV can be recognized. This effect will be discussed in Sec. V D.

### B. $Z^{2+} \cdot Na(3s) \rightarrow Z^{2+} \cdot Na(3p)$

Our results for TX in these collision systems are summarized in Fig. 5 and plotted as reduced cross section  $\sigma/q$  versus reduced impact energy  $E_{red} = E/qm$ . Excellent agreement between theoretical (Ref. [29] and this work) and experimental results (Ref. [10] and this work) is found. However, one has to consider that in Figs. 4–6 experimental emission cross sections are compared with pure TX cross sections and a

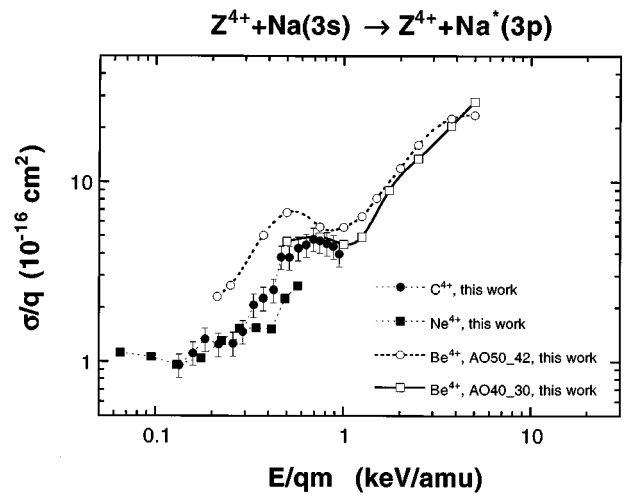


FIG. 6. Measured NaI (589.0+589.6 nm) emission and calculated Na(3*p*) excitation cross sections plotted as reduced cross section  $\sigma/q$  vs reduced impact energy  $E/qm$  for impact of various quadruply charged ions. Experimental data ( $E$ ): ●:  $C^{4+}$  (this work); ■:  $Ne^{4+}$  (this work). Calculated data ( $T$ ) are for  $Be^{4+}$  projectiles but using two different AO basis sets (cf. Table I and text): ○: AO50-42 this work; □: AO 40-30 this work.

proper consideration of cascade contributions might increase the deviation between theories and experiments.

Below  $E_{red} = 0.5$  keV/amu results from AO29-21 are used in Fig. 5 rather than the "larger" calculation AO49-18 (cf. Table I). The basis of AO29-21 includes only the most important AO states [dominant SEC final shell  $n=3$  and  $Na(3s)$ ,  $Na(3p)$  on target center] completed by a rather large number of PS states in order to allow the formation of transient molecular orbitals. Reasons why such a basis gives advantages over larger expansion with more AO states were already discussed in Sec. III. At  $E_{red} = 0.5$  keV/amu results of both basis sets agree within 10%. Again, a distinct structure in the TX cross section can be recognized.

### C. $Z^{4+} \cdot Na(3s) \rightarrow Z^{4+} \cdot Na(3p)$

A theoretical treatment of inelastic processes in ion-atom collisions within the close-coupling approach requires increasing computational effort for larger charge of the projectile, because much more states with higher  $n, l$  quantum numbers are involved. Therefore, such calculations might easily suffer from too small basis sets, which have to be chosen under the constraints of available computer capacity. On the other hand, the inclusion of UA states on the projectile center seems to be less important or even redundant, because of the large overlap with the actual AO states representing SEC channels. From this point of view an inclusion of AO states only on the projectile center should be a good choice (cf. Table I for AO40-30).

Comparison of theoretical results from two different expansion sets with our experimental data for  $C^{4+}$  and  $Ne^{4+}$  is shown in Fig. 6. Above  $E_{red} \geq 1.5$  keV/amu results of both expansions AO40-30 and AO50-42 (cf. Table IV) are equal within 10%. However, below  $E_{red} \leq 1$  keV/amu theoretical results deviate from each other as well as from the experimental data considerably. For  $E_{red} \leq 0.5$  keV/amu the

AO40-30 expansion containing only AO states on the projectile center does not deliver reasonable results (which are therefore not shown in Fig. 6). Enlarging the basis on both centers (AO50-42) improves the agreement, but a deviation of almost a factor of 2 with respect to the experimental values remains at the lower impact energies.

We believe that these problems of the present calculations are probably not only due to the choice of basis, but mainly the inadequacy of the pseudopotential used (cf. the interesting discussion about pseudopotentials by Jain and Winter [27]). Although our calculations for the other collision systems are based on the same pseudopotential [24] and deliver quite good results, the sensitivity to the pseudopotential used will certainly increase considerably with  $q$ . Further investigations concerning this problem are under way. Despite these problems a similar structure of the TX cross section as for the other projectiles is found in both the theoretical as well as the experimental results (cf. Fig. 6 and Ref. [30]).

#### D. Discussion of structure in TX cross section scaling with respect to $q$

Figure 7(a) summarizes our calculated TX cross sections for the three different projectiles  $Z^{q+}$  ( $q=1,2,4$ ). In addition calculated (reduced) total SEC cross sections  $\sigma/q$  are shown for comparison. A striking feature of Fig. 7(a) is the appearance of a pronounced ‘‘plateau structure’’ in the TX cross section exactly between  $E/m=1.5$  and  $3.5$  keV/amu independent of projectile charge. Not only the position of this structure is independent of the initial projectile charge but also the absolute cross section value. The TX cross section in this impact energy range seems to be determined only by the target, but remains completely independent of the projectile species. The appearance of a plateau structure in the AO calculations is also not very sensitive to the chosen basis (as are the absolute cross-section values) and will appear as long as at least the dominantly populated SEC shell and the lower bound Na states are included in the calculation (cf. Fig. 6 for comparison of AO calculations with different basis).

For impact energies especially in the region of the plateau TX is strongly suppressed by the dominant SEC reaction, whereas for higher impact energies, where SEC starts to decrease sharply, TX becomes decoupled from SEC [7]. This can be deduced from comparing results from AO calculations with the same number of Na target and different number on SEC projectile channels. Especially a pure one-center expansion (not shown) neglecting all SEC channels produces for  $E=20$  keV within 10% the same cross section value as the presented ‘‘full’’ AO calculation. In the impact energy range from 1 to 5 keV, however, the results of the one-center expansion overestimates the cross section by a factor 5. The cross section of such a one-center expansion does not show any plateau structure, but produces a broad maximum around 4 keV/amu. At this impact energy the direct Na( $3s-3p$ ) excitation by the disturbing electric field of the projectile is most effective, but will be suppressed because of SEC. The plateau structure appears by including SEC channels in an AO expansion and might, therefore, just be a remainder of the primary cross section maximum found in the one-center expansion. The increase of the TX cross section for impact energies above the plateau region can be explained by more

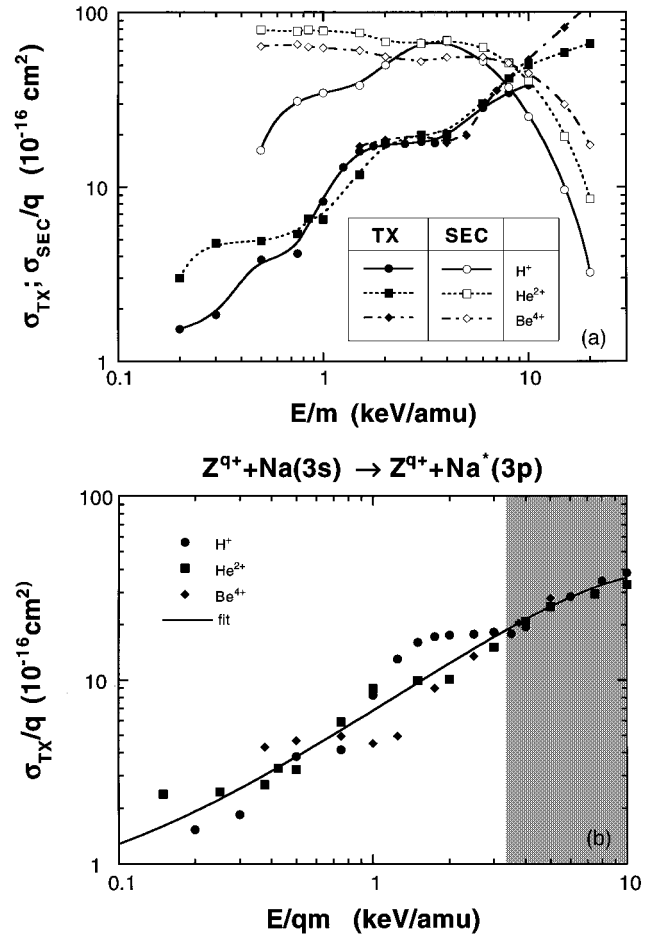


FIG. 7. (a) Calculated Na( $3p$ ) excitation cross sections  $\sigma_{TX}$  (full symbols) and calculated (reduced) single electron capture cross sections  $\sigma_{SEC}/q$  vs impact energy per atomic mass unit  $E/m$  for impact of  $H^+$  (circles),  $He^{2+}$  (squares) and  $Be^{4+}$  (diamonds) on Na( $3s$ ). (b) Calculated (reduced) Na( $3p$ ) excitation cross sections  $\sigma_{TX}/q$  vs reduced impact energy  $E/qm$  for impact of  $H^+$  (circles),  $He^{2+}$  (squares) and  $Be^{4+}$  (diamonds) on Na( $3s$ ). Also shown is a least square fit (full line) to all reduced cross sections. For  $E_{red} \geq 3.5$  keV/amu (shaded region) all cross sections follow a  $\sigma_{TX}/q = f(E/qm)$  scaling relation.

and more decoupling of TX from SEC.

Furthermore, it is interesting to note that the excitation energy of the  $3s-3p$  transition  $\Delta E = 2.1$  eV corresponds to an electron velocity of  $v_e \approx 0.39$  a.u., which roughly coincides with the projectile velocity (0.245–0.374 a.u.) in this impact energy range (cf. also [27]). Of course further investigations of the TX process in the presented and especially in collision systems involving other target atoms will be necessary to establish a clear picture for such plateau structures in TX cross sections.

In Fig. 7(b) the scaling relation  $\sigma/q$  versus  $E_{red} = E/qm$  [11,12,17] for TX is applied to our calculated results. One can distinguish between two impact energy regions. For  $E_{red} \geq 3.5$  keV/amu the scaling relation is almost perfectly fulfilled for all regarded projectiles. Below that value the scaling is destroyed mainly because of the  $q$ -independent plateau structure, which appears at fixed  $E/m$ . However, for higher  $q$  projectiles rough estimates of TX cross sections

seem to be possible within an error of  $\pm 50\%$  by applying the fit curve shown in Fig. 7(b).

## VI. SUMMARY

Experimental and theoretical data for Na( $3p \leftarrow 3s$ ) excitation in collisions of Na( $3s$ ) atoms with slow ( $v < 1$  a.u.) singly and multiply charged ions have been presented and exhibit the following general trends. Target excitation cross sections, if compared at the same impact velocity, do not strongly depend on projectile charge state and species and exhibit a pronounced structure. Projectile ions in higher charge states are generally somewhat less efficient in excit-

ing the alkali atoms than the lower charged ones. The usual TX scaling  $\sigma/q$  versus reduced impact energy  $E/qm$  is not appropriate at our comparably low impact energies. Our calculations indicate a strong coupling between the TX channel and the by far dominant SEC channel, which seems to be responsible for the observed structure in the TX cross section.

## ACKNOWLEDGMENTS

This work has been supported by Fonds zur Förderung der wissenschaftlichen Forschung (Projekt No. P9459-PHY).

- 
- [1] E. Wolfrum, F. Aumayr, D. Wutte, HP. Winter, E. Hintz, D. Rusbüldt, and R. P. Schorn, *Rev. Sci. Instrum.* **64**, 2285 (1993).
  - [2] J. Schweinzer, E. Wolfrum, F. Aumayr, M. Pöckl, HP. Winter, R. P. Schorn, E. Hintz, and A. Unterreiter, *Plasma Phys. Controlled Fusion* **34**, 1173 (1992).
  - [3] F. Aumayr, R. P. Schorn, M. Pöckl, J. Schweinzer, E. Wolfrum, K. McCormick, E. Hintz, and HP. Winter, *J. Nucl. Mater.* **196–198**, 928 (1992).
  - [4] R. P. Schorn, E. Hintz, D. Rusbüldt, F. Aumayr, M. Schneider, E. Unterreiter, and HP. Winter, *Appl. Phys. B* **52**, 71 (1991).
  - [5] R. P. Schorn, E. Wolfrum, F. Aumayr, E. Hintz, D. Rusbüldt, and HP. Winter, *Nucl. Fusion* **32**, 351 (1992).
  - [6] R. K. Janev, J. J. Smith, F. Aumayr, D. Wutte, M. Schneider, HP. Winter, and J. Schweinzer, *Atomic Collision DataBase for Li Beam Interaction with Fusion Plasmas* (IAEA International Atomic Energy Agency, 1993).
  - [7] J. Schweinzer, D. Wutte, and HP. Winter, *J. Phys. B* **27**, 137 (1994).
  - [8] A. M. Ermolaev, R. N. Hewitt, R. Shingal, and M. R. C. McDowell, *J. Phys. B* **20**, 4507 (1987).
  - [9] K. Kadota, D. Dijkamp, R. L. van der Woude, P. G. Yan, and F. J. deHeer, *J. Phys. B* **15**, 3297 (1982).
  - [10] A. R. Schlatmann, R. Hoekstra, H. O. Folkerts, and R. Morgenstern, *J. Phys. B* **25**, 3155 (1992).
  - [11] W. Fritsch and K. H. Schartner, *Phys. Lett. A* **126**, 17 (1987).
  - [12] R. K. Janev and L. P. Presnyakov, *J. Phys. B* **13**, 4233 (1980).
  - [13] K. Reyman, K. H. Schartner, and B. Sommer, *Phys. Rev. A* **38**, 2290 (1988).
  - [14] M. Anton, D. Dettleffsen, and K. H. Schartner, *Nucl. Fusion Suppl.* **3**, 51 (1992).
  - [15] M. Anton, D. Dettleffsen, K. H. Schartner, and A. Werner, *J. Phys. B* **26**, 2005 (1993).
  - [16] D. Dettleffsen, M. Anton, A. Werner, and K. H. Schartner, *J. Phys. B* **27**, 4195 (1994).
  - [17] R. K. Janev, *Phys. Rev. A* **53**, 219 (1996).
  - [18] E. Wolfrum, R. Hoekstra, F. J. deHeer, R. Morgenstern, and HP. Winter, *J. Phys. B* **25**, 2597 (1992).
  - [19] F. Aumayr, M. Fehring, and HP. Winter, *J. Phys. B* **17**, 4185 (1984).
  - [20] F. Aumayr, M. Fehring, and HP. Winter, *J. Phys. B* **17**, 4201 (1984).
  - [21] M. Leitner, D. Wutte, J. Brandstötter, F. Aumayr, and HP. Winter, *Rev. Sci. Instrum.* **65**, 1091 (1994).
  - [22] F. Aumayr, G. Lakits, and HP. Winter, *J. Phys. B* **20**, 2025 (1987).
  - [23] W. Fritsch and C. D. Lin, *J. Phys. B* **15**, 1255 (1982).
  - [24] D. Rapp and C. Chang, *J. Chem. Phys.* **58**, 2657 (1973).
  - [25] R. Shingal, B. H. Bransden, A. M. Ermolaev, D. R. Flower, C. W. Newby, and C. J. Noble, *J. Phys. B* **19**, 309 (1986).
  - [26] W. Fritsch, *Phys. Rev. A* **35**, R2342 (1987).
  - [27] A. Jain and T. G. Winter, *Phys. Rev. A* **51**, 2963 (1995).
  - [28] W. Fritsch, R. Shingal, and C. D. Lin, *Phys. Rev. A* **44**, 5686 (1991).
  - [29] R. Shingal, C. J. Noble, and B. H. Bransden, *J. Phys. B* **19**, 793 (1987).
  - [30] F. Aumayr, G. Lakits, and HP. Winter, *Z. Phys. D* **6**, 145 (1987).